Applied Catalysis B: Environmental 180 (2016) 559–568

Contents lists available at ScienceDirect

Applied Catalysis B: Environmental

journal homepage: www.elsevier.com/locate/apcatb

Catalytic conversion of bio-oil in supercritical water: Influence of RuO_2/γ-Al_2O_3 catalysts on gasification efficiencies and bio-methane production

Jude A. Onwudili*, Paul T. Williams

Energy Research Institute, School of Chemical and Process Engineering, The University of Leeds, Leeds LS2 9JT, United Kingdom

ARTICLE INFO

Article history:
Received 12 May 2015
Received in revised form 24 June 2015
Accepted 29 June 2015
Available online 17 July 2015

Keywords:
Hydrothermal gasification
Catalysis
Ruthenium oxide
Bio-methane

ABSTRACT

Catalytic supercritical water gasification of heavy (dewatered) bio-oil has been investigated in a batch reactor in the presence of ruthenium catalysts in the form of RuO_2 on γ-Al_2O_3 support. The reactions were carried out at temperatures of 400 °C, 450 °C and 500 °C and reaction times of up to 60 min using 15 wt% of bio-oil feed. Increased ruthenium oxide loading led to increased carbon gasification efficiencies (CGE) and bio-methane production. Hence, using the 20 wt% RuO_2/γ-Al_2O_3 catalyst, CGE was 97.4 wt% at 500 °C and methane yield reached nearly 30 wt% of the bio-oil feed, which gave a CH_4/CO_2 molar ratio of 1.28. There was evidence that the RuO_2 was involved in the initial conversion of the bio-oil to carbon oxides and hydrogen as well as the reduction of the CO_2 to methane via CO methanation. However, competition for CO consumption via the water-gas shift reaction was also possible due to the large presence of water as the reaction medium. This work therefore demonstrates that high concentrations of heavy fraction of bio-oil can be catalytically converted to a methane-rich gas product under hydrothermal conditions at moderate temperatures. The calorific values of the gas product reached up to 54 MJ kg^{-1}, which is nearly 3 times the HHV of the bio-oil feed.

1. Introduction

Fast pyrolysis of biomass is the technology of choice for the preferential production of bio-oil. This liquid product is a dark brown viscous mixture of water and a variety of many chemical compounds, which gives it a characteristic smoky odour. Generally, crude bio-oil, freshly obtained from the pyrolytic process consists of moisture, carboxylic acids, carbohydrates, alcohols, ketones, aldehydes, phenolics, furfurals and other water- insoluble compounds formed mainly from the lignin fraction of biomass [1]. Fast pyrolysis may be regarded as a biomass pre-processing technology to produce a liquid bio-oil which is much easily adaptable to further processing than the original solid biomass and contains about 10 times higher energy density compared to raw biomass [2]. Hydrothermal processing, which takes place in high-temperature, high-pressure water conditions, can be a viable technology for the conversion of bio-oil to more useful products including biogas and liquid biofuels. Therefore, fast pyrolysis can be used to solve one of the challenges of hydrothermal gasification of biomass, which is the difficulty in delivering solid biomass feedstock continuously into a hydrothermal reactor [3–6].

The physical characteristics and chemical composition of crude bio-oil renders it directly unusable as liquid fuels in conventional engines without modifications of the bio-oil or the engines. This is due to problems of massive acidic and hot alkali corrosion, significant wear, solid deposition and poor ignition [7–8]. Moreover, crude bio-oils have relatively low calorific values of between 16 and 19 MJ kg^{-1} compared with conventional fuels such as heavy oil (40 MJ kg^{-1}) for power plants and would result in poor electricity production efficiency. The performance of bio-oils can be improved by mixing with methanol and other cetane- improving additives [8], however at increased costs. A number of upgrading processes and technologies have been proposed to improve the qualities of bio-oil. These include hydrodeoxygenation (HDO) using molecular hydrogen or hydrogen source and a variety of catalysts, two-stage pyrolysis-catalytic upgrading processes, esterification and a host of physical processes including hot filtration, sedimentation and centrifugation [9]. HDO has been proposed for the conversion of low-oxygen heavy bio-oil fractions for liquid fuels production, while the aqueous fraction could be reformed to hydrogen for the HDO process [2,10].

* Corresponding author. Fax: +44 113 246 7310.
E-mail address: j.a.onwudili@leeds.ac.uk (J.A. Onwudili).

http://dx.doi.org/10.1016/j.apcatb.2015.06.058
0926-3373/

Van Rossum and co-workers [11–12] have been investigating conventional catalytic gasification at temperatures between 500 and 900 °C as a way of adding more value to pyrolysis oils. In addition, catalytic reforming of the separated aqueous fractions of bio-oil has become an active research area in the last few years. Technologies such as aqueous-phase reforming, supercritical water gasification (SCWG), steam reforming and autothermal reforming have all been investigated. Due to the high water contents of the raw bio-oil and particularly, its separated water-soluble fraction, hydrothermal conversion is seen a suitable technology. However, current methods of precipitating the insoluble fraction by adding more water to the bio-oil would generate significant amounts of process water, especially with water additions of up to 5 times the mass of bio-oil [13–14]. The process water would need to be further valorised depending on its carbon content or treated before disposal.

A number of researchers have investigated the catalytic hydrothermal conversion of the aqueous fraction of bio-oil to hydrogen- or methane-rich syngas. For example, Penninger and Rep [15] have reported the SCWG of aqueous wood condensate in a tubular flow reactor. The reaction, which was carried out 650 °C and 28 MPa, gave a hydrogen-rich gas and resulted in about 90% carbon gasification. Hydrogen selectivities increased with addition of <0.1% Na_2CO_3 to promote water–gas shift (WGS) reaction. Similarly, Di Blasi et al. [13] carried out the SCWG of diluted wastewater collected from the downstream of an updraft wood gasification plant. The SCWG process carried out at temperatures in the range of 450–548 °C yielded TOC conversions of between 30 and 70%. Vispute and Huber [16] reported the aqueous-phase reforming of water-soluble fraction of bio-oil at 265 °C, 5.5 MPa with Pt-based catalyst, which yielded carbon gasification efficiency of just 35%, however the product gas gave 45% selectivity for alkanes at a WHSV of 0.96 h^{-1}. In addition, Chakinala et al. [17] targeted hydrogen production from aqueous phase of bio-oil with a range of metal catalyst, including nickel, ruthenium, rhodium, platinum and palladium. They found that ruthenium gave the highest gasification efficiency (GE), while palladium gave the highest selectivity for hydrogen. All these reported cases involved using aqueous-phase fractions with low concentrations e.g. 0.65–3.1 wt% TOC [13], 4 wt% organic [15], 1% TOC [16] and 5 wt% [17]. They also showed that attempts to increase feed concentrations resulted in poor conversion difficulties due to tar formation, reactor pulling and clogging of the pump outlets during continuous operation. In addition, high biomass feedstock concentrations in batch reactors have resulted in low carbon gasification efficiencies and reduction in hydrogen yields [18–20].

While, it may therefore be beneficial to develop appropriate hydrothermal technologies for upgrading bio-oil, via either complete gasification or reforming, the former appears to offer a simple alternative of transforming the complex bio-oil into simple gases. Such an approach may be used to upgrade raw unseparated bio-oil completely to useful syngas for direct use or adapted to produce syngas for the production of cleaner liquid fuels via Fischer–Tropsch synthesis. Conversion of bio-oil to combustible gases such as methane and hydrogen via hydrothermal gasification will enable a rapid market penetration due to the existing markets and infrastructures for these products. Hence, in this work, a sample of the heavy fraction of bio-oil has been subjected to supercritical water gasification (SCWG) conditions in a batch reactor and in the presence of ruthenium oxide catalysts. The aim of this work was to investigate the feasibility of complete gasification of high concentration of bio-oil in supercritical water with the aid of the stable RuO_2/γ-Al_2O_3 catalysts. The results of this work would provide important data that will contribute to further commercial development of hydrothermal conversion of bio-oil as a viable alternative to existing technologies.

Table 1
Characteristics of the heavy fraction of bio-oil.

Parameters	Value
Carbon (wt%)	41.0
Hydrogen (wt%)	6.10
Sulphur (wt%)	<0.01
Nitrogen (wt%)	<0.01
Oxygen* (wt%)	52.9
Moisture content (wt%)	3.20
Calorific Value (MJ/kg)	20.0
Density (g/cm^3)	1.22
Kinematic Viscosity at 20 °C (mm^2/s)	131
Dynamic Viscosity at 20 °C (mPa s)	159
PH	3.10
Solubility in dichloromethane (%)	59.5

* Calculated by difference

Table 2
Characteristics of the ruthenium oxide-alumina catalysts.

Parameters	Value		
	5 wt%	10 wt%	20 wt%
BET surface area (m^2/g)	8.54	8.06	7.97
Pore volume (cm^3/g)	0.027	0.023	0.025
Pore adsorption diameter	12.7	11.2	12.4
Pore desorption diameter	15.4	15.3	16.5
% Ruthenium metal	4.05	7.48	15.1

2. Experimental

2.1. Materials

The sample of bio-oil was obtained via fast pyrolysis at 710 °C in a fluidized bed reactor with a short gas residence time of <1 s. The bio-oil was then subjected to distillative separation and centrifugation to reduce its moisture content to 3.2 wt%. The water content was reduced to this level as a precaution to prolong the shelf-life (stability) and ensure consistent composition of the bio-oil. The characteristics of the bio-oil are presented in Table 1. Commercial ruthenium oxide—gamma alumina (RuO_2/γ-Al_2O_3) catalysts containing 5 wt%, 10 wt% and 20 wt% of the ruthenium oxide were used in these tests. The catalysts and bio-oil sample were obtained from Catal Ltd., a UK-based SME. The catalysts were in the form of 1 mm pellets but were pulverized and sieved to <125 μm particle size before use. XRD analysis confirmed that the ruthenium was present as ruthenium (IV) oxide (RuO_2). The catalysts were pulverized and sieved to ≤120 nm before characterization and use. The characteristics of the catalysts are presented in Table 2. Dichloromethane (99% purity) used as extraction solvent was purchased from Sigma–Aldrich, UK.

2.2. Methods

The container holding the bio-oil was agitated on a laboratory shaker for 10 min before samples were taken and weighed. In each test, 17 ml of deionized was added into a 75 ml Inconel batch hydrothermal reactor [21] followed by 1.0 g of the RuO_2/γ-Al_2O_3 catalyst (when used). The mixture of water and catalyst was stirred with a glass rod prior to adding 3.0 g of bio-oil. The bio-oil loading was therefore 15 wt% in each case. After loading, the reactor was sealed, purged with nitrogen gas for 10 min and pressurized to 1 bar with the nitrogen gas prior to heating. The heater was placed in a vertical ceramic 1.5 kW knuckle heater and heated to the designated temperatures of 400 °C, 450 °C and 500 °C at an average heating rate of 21 °C min^{-1}. Majority of the tests were carried out for 60 min reaction time at the designated temperatures to investigate the effect of reaction temperature and ruthenium

loading. To investigate the influence of reaction time, experiments were carried out at 0, 30 and 60 min at 500 °C with the 20 wt% RuO_2/γ-Al_2O_3. During the batch reactions, the operating pressures varied depending on reaction temperatures, reaction time and percentage of ruthenium in the catalyst, ranging from 26.5 MPa at 400 °C and up to 40 MPa at 500 °C. At the end of the reaction, the reactor was quickly withdrawn from the heater and rapidly cooled to room temperature with a combination of a fan and compressed air. On cooling, the pressure exerted by the product gas was noted prior to gas sampling for gas chromatographic analysis.

2.2.1. Gas products analysis

The gas products obtained from the reactions were sampled via gas-tight plastic syringes and immediately analysed using gas chromatography [20,22]. Briefly, permanent gases including hydrogen, nitrogen and carbon monoxide were analysed using a column fitted on a GC with a thermal conductivity detector (GC-TCD). Carbon dioxide was analysed on a separate column used in a different GC/TCD. Finally, hydrocarbon gases including methane, ethene, ethane, propene, propane, butane, butene and butadiene were separated on a column in a GC fitted with a flame ionization detector (FID). Gas analyses were carried out in triplicates with less than 1% standard deviation for each gas component. The results of the analyses were obtained in volume percent and converted to moles of each gas using ideal gas equation and Henry's Law.

2.2.2. Liquid and solid sampling

After gas analysis, the remaining gas products were discharged and the reactor opened to sample its liquid and solid contents. Prior to sampling, 100 μL of 2-hydroxyacetophenone (internal standard) was added to the reactor, followed by dichloromethane (DCM) extraction solvent. The contents of the reactor were quantitatively transferred onto a filtration system to separate the solid residues from the liquid products. More DCM and deionized water were used to wash the reactor and filter paper until clear.

2.2.3. Solid analysis

The solid residues were homogenized with a laboratory mortar and pestle before further analysis. Firstly, the solid residues were analysed for char contents by ashing at 550 °C overnight. The difference in weight between the solid residue and the ash was taken as the weight of char. Furthermore, the fresh catalysts, the solid residues and the calcined catalyst (ash obtained from the solid residues) were all analysed by an X-ray diffractometer (XRD) to check for the alumina and ruthenium oxide phases [23]. In addition, the fresh catalyst and calcined catalysts were characterised by scanning electron microscope—energy dispersive X-ray spectroscopy (SEM-EDXS). The instrumentation used was a Jeol JSM-6610LV Scanning Electron Microscope coupled to an Oxford Instruments INCA X-max80 EDS system. Prior to analyses, the powdered catalyst samples were gold-coated (30 nm) using a Quorum Q150RS sputter coating unit. Secondary electron micrographs for the samples were recorded using an accelerating voltage between 15 kV and 30 kV. EDXS semi-quantitative analysis for the catalyst samples were undertaken using an accelerating voltage of 20 kV, an aperture of 2 and a beam spot size of 50.

2.2.4. Liquid analysis

The mixtures of aqueous and organic (DCM) fractions obtained after the filtration procedure were separated by liquid–liquid extraction technique. Each mixture was carefully transferred into a separation flask, equilibrated and left for 30 min to separate into the organic and aqueous phases. Residual water-soluble products (WSP), in the aqueous fractions remaining after the extraction of the organic compounds, were determined by evaporation and gravimetry. In the procedure, 50 ml of the homogenous aqueous fraction was evaporated on a pre-weighed porcelain crucible on a water-bath and dried in a desiccator overnight. The DCM fraction was withdrawn and the extraction procedure repeated two more times. The organic fraction was analysed on a GC coupled to an MS/MS system [21]. Briefly, a Varian CP-3800 gas chromatograph coupled with a Varian Saturn 2200 mass spectrometer (GC/MS/MS) was used. The oil components were separated on a 30 m DB-5 equivalent column. For the GC/MS/MS analysis, 2 μl of each DCM extract was injected into the GC injector port at a temperature of 290 °C; the oven programme temperature was 35 °C for 8 min, then ramped to 120 °C at 5 °C min^{-1} heating rate, held for 1 min and ramped at 4 °C min^{-1} to 210 °C and finally ramped at 20 °C min^{-1} to 280 °C (total analysis time of 55.5 min). The transfer temperature line was at 280 °C, manifold at 120 °C and the ion trap temperature was held at 200 °C. The MS system was operated in the Electron Impact (EI) mode. The compounds present in the extracts were quantified by internal standard method with the added internal standard.

3. Results and discussions

3.1. Effect of reaction time at 500 °C

In this work, considering that gas yields consistently increased with temperature, it was decided that the influence of reaction time be tested at the highest temperature of 500 °C. The tests were carried out at 0, 30 and 60 min reaction hold times using the 20 wt% RuO_2/γ-Al_2O_3 catalyst. As shown in Table 3, at 0 min total gas yield was 64.3 wt% but this increased to 86.2 wt% after 30 min and then finally to 96.4 wt% after reacting for 60 min. These results showed that longer reaction times at the designated temperatures were required for increased gasification of the bio-oil, which justified the use of 60 min reaction time for the majority of this present work.

3.2. Effect of ruthenium loading and reaction temperature

3.2.1. Product yields

Table 3 shows that gas production increased with the increase in reaction temperatures (400–500 °C) and ruthenium oxide loading, i.e. the percentage of RuO_2 in the catalyst (5–wt%). Yamamura et al. [24] showed that water participates in the catalysis by RuO_2 and this has been taken into consideration in calculating the mass balances. The increase in gas yields corresponded to decreases in the yields of other products, such as WSP, oil and char. The highest conversion of bio-oil to gas were observed using 20 wt% ruthenium catalyst at the respective temperatures, so that at 500 °C, about 96 wt% gas yield was obtained with this catalyst. The increase in bio-oil gasification was less dramatic between 450 °C and 500 °C compared to the increase in gas production from 400 °C to 450 °C. Without any catalysts at 400 °C, there was nearly an equal distribution of the bio-oil into oil, gas and solid products. However, as the temperature increased, gas products became more dominant at 450 °C and 500 °C, without catalysts. There was an interesting trend with regards to the WSP, which appeared to increase between the non-catalytic reactions and the reactions with 5 wt% RuO_2/γ-Al_2O_3, after which, it consistently decreased with increased ruthenium loading.

Considering the reduction in the yield of char between the non-catalytic tests and the reaction involving 5 wt% catalyst, it could be suggested that the ruthenium catalyst was capable of suppressing char formation by breaking CC bonds in the bio-oil components [24–27]. In the hydrothermal medium, CC bond cleavage would result in forming short-chain products and intermediates which became increasingly gasified [24]. Sato et al. [25] found that Ru/γ-alumina gave the highest conversion of alkylphenols as lignin model compounds during SCWG tests at 400 °C, in the presence

Table 3
Product yields and mass balances from catalytic SCWG of heavy fraction of bio-oil.

RuO_2 loading in catalyst	Temperature (°C)	Reaction time (min)	WSP (wt%)	Oil (wt%)	Char (wt%)	Gas (wt%)	Balance (%)
No catalyst	400	60	3.96	30.5	33.6	31.4	99.5
Ru/Al_2O_3 5 wt%	400	60	6.75	21.3	10.1	55.8	93.9
Ru/Al_2O_3 10 wt%	400	60	4.73	14.3	6.72	69.9	95.6
Ru/Al_2O_3 20 wt%	400	60	0.71	5.67	6.19	82.5	95.0
No catalyst	450	60	2.46	26.3	26.0	42.3	97.0
Ru/Al_2O_3 5 wt%	450	60	7.65	16.0	10.0	64.9	98.5
Ru/Al_2O_3 10 wt%	450	60	1.58	4.29	9.73	80.1	95.7
Ru/Al_2O_3 20 wt%	450	60	0.65	2.63	4.53	91.4	99.2
No catalyst	500	60	0.92	24.5	22.3	50.9	98.6
Ru/Al_2O_3 5 wt%	500	60	5.96	4.90	8.76	76.2	95.9
Ru/Al_2O_3 10 wt%	500	60	0.59	2.89	5.41	90.8	99.7
Ru/Al_2O_3 20 wt%	500	60	0.58	1.15	3.04	96.4	101
Ru/Al_2O_3 20 wt%	500	0	4.01	15.6	11.6	64.3	95.5
Ru/Al_2O_3 20 wt%	500	30	2.96	4.15	4.38	86.2	97.7

of supported noble metal (Ru, Rh, Pt, and Pd) catalysts. Yamamura et al. [24] used unsupported RuO_2 as catalyst for the SCWG of low concentrations (~ca. 3.33 wt%) of biomass model compounds, paper sludge and sewage sludge at temperatures of up to 500 °C and found that hydrogen, methane and carbon dioxide were the main gas products. The authors reported complete gasification of cellulose and glucose, along with high conversions of N- and S-heterocyclic compounds, and proposed a mechanism involving a redox cycle between Ru(IV) and Ru(II).

Oil yield was highest in the non-catalytic reactions at each reaction temperature, but consistently decreased as the reaction temperaures increased. At 400 °C, oil yields was 31.5 wt% in the absence of catalysts and decreased by 32%, 55% and 82% respectively, in the presence of 5 wt%, 10 wt% and 20 wt% RuO_2/γ-Al_2O_3 catalyst. Similarly at 450 °C and 500 °C, oil yields were 26.3 wt% and 24.5 wt% respectively, during the non-catalytic reaction and decreased steadily as the ruthenium oxide loading in the catalysts increased. Indeed, at 20 wt% ruthenium loading, oil yield decreased to 1.15 wt% of the bio-oil feed at 500 °C. The presence of increasing ruthenium loading in the catalysts led to steady decline in the yields of char products at each reaction temperature. Similar to the trend in oil yields, the yield of char decreased as the reaction temperature increased, so that with the 20 wt% RuO_2/γ-Al_2O_3, char yield was 6.19 wt% at 400 °C, which decreased to 4.5 wt% and 1.04 wt% at 450 °C and 500 °C, respectively.

3.2.2. Detailed analysis of gas products

3.2.2.1. Carbon gasification efficiency (CGE). The gas yields were determined both by carbon gasification efficiency (CGE) and the actual yields of individual gases. CGE was calulated as follows;

$$\text{CGE}(\%) = \frac{\text{Mass of carbon in the gaseous products} \times 100}{\text{Mass of carbon in bio} - \text{oil feed}} \quad (1)$$

Fig. 1 shows the trends in CGE during the SCWG of bio-oil with and without the ruthenium catalysts. Clearly, this figure mirrors the trend in the product distribution discussed above, showing the conversion of the bio-oil carbon into gas products. The CGE increased dramatically between the non-catalytic runs and the catalytic tests using the 5 wt% RuO_2/γ-Al_2O_3. Similar, increase in CGE can also be observed between the values obtained from the tests with 5 wt% and 10 wt% catalysts, while the increase in CGE narrowed between the 10 wt% and 20 wt% catalysts in this work. Hence, doubling the ruthenium loading from 10 wt% to 20 wt%, though gave improved CGE values but not by a lot, suggesting that the bio-oil feed amount became a limiting factor. The highest CGE obtained from this work was 97.4 % at 500 °C using the 20 wt% catalyst, while the 10 wt% catalyst gave its highest CGE of 91.5% at the same temperature. Elliott et al. [28] reported that ruthenium catalyst gave up to 99.8% carbon conversion in terms of chemical oxygen demand, during the aqueous-phase reforming of process waters obtained from hydrothermal liquefaction of algae, with a biogas composition of ~60% CH_4, 30% CO_2, 5% NH_3, and 2% H_2.

The effect of increasing temperature was very obvious from the CGE results at all temperatures but with interesting trends for the non-catalytic and the catalytic SCWG with the 5 wt% RuO_2/γ-Al_2O_3. The non-catalytic test showed a steeper increase in CGE from 400 °C to 450 °C and then slowed between 450 °C and 500 °C. In contrast, the trend in CGE shows a slow increase between 400 °C and 450 °C in the the presence of 5 wt% RuO_2/γ-Al_2O_3, while catalytic activity seemed to increase from 450 °C to 500 °C. On one hand, this could be explained by the stabilization of the reaction products, possibly due to the formation of char during the non-catalytic tests, so that once char was formed no significant gasification could occur. On the other hand, it would appear that the rate of bio-oil solubilization was faster than catalytic activity for the 5 wt% catalyst but that the catalysts was able to gasify even the char products at higher temperatures.

3.2.2.2. Gas compositions and yields. The major components in the gas products included hydrogen, methane, carbon dioxide, carbon monoxide and hydrocarbon gases (C_2–C_4). The yields of the C_2–C_4 gases were relatively low compared to the others, so that their yields have been combined in this report. Fig. 2 presents the volume

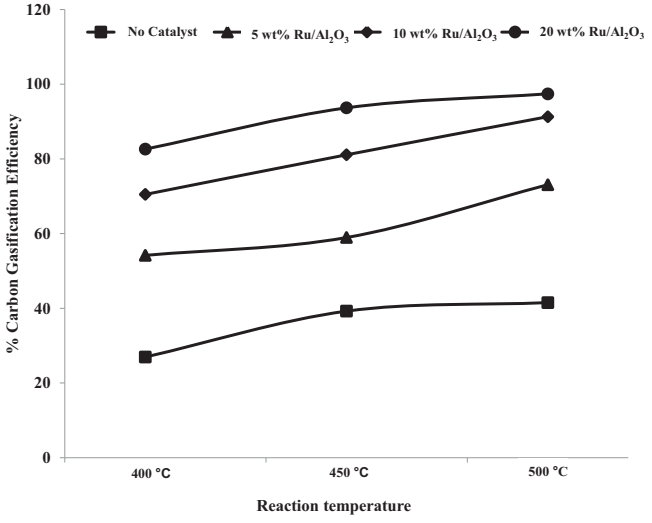

Fig. 1. Carbon gasification efficiencies (CGE) from bio-gasification in relation to ruthenium catalyst loading.

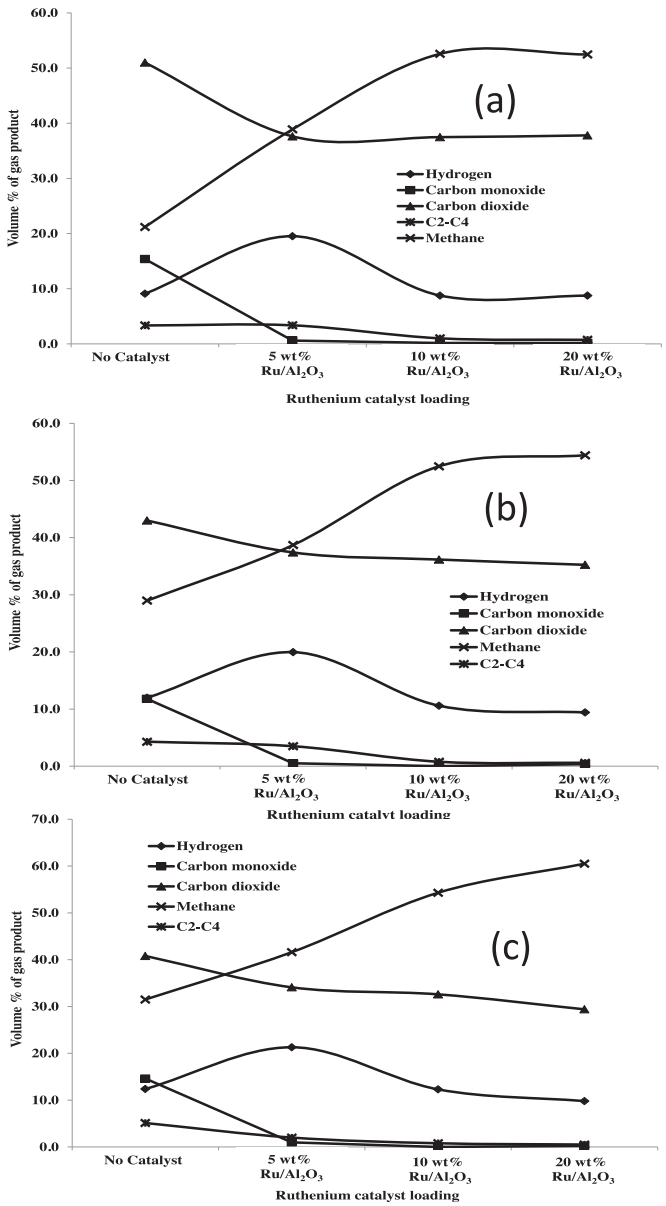

Fig. 2. Volume percent yields of gas components in relation to temperatures and ruthenium loading in the catalysts: (a) 400 °C; (b) 450 °C; (c) 500 °C.

percent yields of the components in the gas products in relation to catalyst loading and reaction temperature. In the absence of catalyst, carbon dioxide was the dominant reaction product at all temperatures. However, in the presence of the ruthenium oxide catalyst, the volume percent of methane increased and overtook that of CO_2. High yields of methane have been reported during the supercritical water gasification of different biomass samples in the presence of ruthenium catalyst [10,17,28]. Interestingly, Fig. 2 shows that the point at which methane overtook CO_2 shifts leftward as temperature increased, indicating a positive influence of methanation rate i.e. the catalytic activity of the ruthenium oxide catalyst for methanation increased with increasing temperature. In terms of volume percent, the three predominant gases were carbon dioxide, methane and hydrogen. The volume percent of hydrogen was highest with 5 wt% RuO_2/γ-Al_2O_3 loading at each temperature. The trend in hydrogen yield was similar at all temperatures investigated in this work; it was between 8 and 10 vol.% for the uncatalysed test but rose to between 18 and 20 vol.% in the presence of the 5 wt% RuO_2/γ-Al_2O_3, and then fell and stabilized at about 10 vol.% with the 10 wt% and 20 wt% RuO_2/γ-Al_2O_3 catalysts. Using 2.0 g Ru/amorphous Al_2O_3 catalysts, Byrd et al. [26] reported the complete conversion of 1.0 wt% glucose solution to yield 12 mol H_2/mol of glucose at 700 °C after 2 s reaction time in a tubular reactor. The differences in the results reported by Byrd et al. [26] and this work may be due to differences in feed loading, reactor temperature, reaction time, catalyst composition and catalyst/feed ratio. It would appear that using ruthenium metal at higher temperatures [26,29] favoured hydrogen production, while using RuO_2, moderate temperatures and long reaction times in this present study favoured methane production. Although, the highest RuO_2/feed mass ratio (for the 20 wt% RuO_2/γ-Al_2O_3 catalyst) in this work was 1:15, the results were comparable to those of Yamamura et al. [24], who used a RuO_2/feed ratio of 1:5 in their work, which may indicate the contribution of the support.

Byrd [26,29] explained that the gasification mechanism for hydrogen production included adsorption of glucose on the catalyst surface, followed by dehydration, and then CC and C—O bond cleavages followed by water-gas shift reaction. However, the main reaction mechanism of CO_2 methanation with ruthenium catalysis have been variously reported in literature [30–31] to be via a two-step hydrogenation or reduction of CO_2 to CO and then to methane;

$$CO_2 + H_2 \Leftrightarrow CO + H_2O \quad (2)$$

$$CO + 3H_2 \Leftrightarrow CH_4 + H_2O \quad (3)$$

Therefore, 'dry' methanation reaction is heavily dependent on the partial pressures of CO_2 and hydrogen. However, in this work, the large presence of water, could lead to competition between CO methanation and CO water-gas shift (WGS) to hydrogen, which is the equilibrium reaction in Eq. (2). Gas products in the presence of ruthenium contained at least 10 vol.% hydrogen gas in all cases. This fairly high volume concentration of hydrogen gas and the little or no CO in the presence the catalysts, may suggest that the consumption of CO during methanation was faster that the reduction of CO_2–CO [30] according to Eq. (2), which may be explained by the competition for CO for methanation and hydrogen production via WGS. Therefore, it could be the case that the presence of water affected the equilibrium of reaction 2 more than that of reaction 3.

Fig. 3 presents the weight percent yields of the gas component on the basis of the bio-oil feed, which shows that carbon dioxide and methane increased almost linearly with increasing ruthenium loading at 400 °C. However, at 450 °C and 500 °C, there was a linear increase of carbon dioxide and methane yields from the non-catalytic test up to the presence 5 wt% RuO_2/γ-Al_2O_3, then the yields of the gases slowly increased when the ruthenium oxide loading was increased up to 20 wt%. Substantial yield of carbon monoxide of up to 5.3 wt% of the gas product obtained at 500 °C, was observed in the absence of the ruthenium oxide catalysts. However, the presence of the catalyst led to nearly complete disappearance of CO, suggesting occurence of methanation reaction. The yields of C_2–C_4 gases also experienced similar trends comparable with the trends in CO yields.

Fig. 4 shows the plot of the molar yield ratios of methane to carbon dioxide. The uncatalysed reaction show a linear increase in CH_4/CO_2 ratio with increasing temperature, which increased dramatically in the presence of 5 wt% catalyst, and reached the highest ratio of 1.28 at 500 °C. The 10 wt% and 20 wt% catalyst, produced CH_4/CO_2 ratios greater than unity (1) at all temperatures, indicating that the higher loadings of ruthenium oxide favoured CO_2 methanation. The CH_4/CO_2 ratio for the 10 wt% and 20 wt% RuO_2/γ-Al_2O_3 are clearly similar at both 400 °C and 500 °C, only differing slightly at 450 °C. The similar ratios at these temperatures could be attributed to the equilibrium limitation imposed by the competing reactions

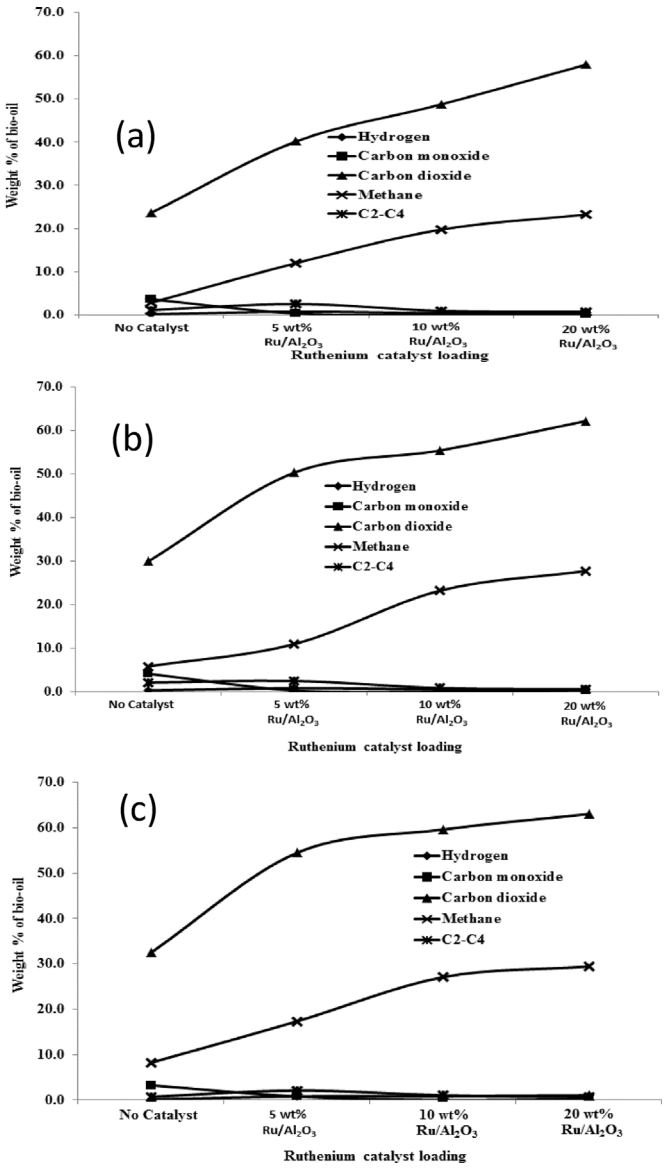

Fig. 3. Weight percent yields of gas components in relation to temperature and ruthenium loading in the catalyst: (a) 400 °C; (b) 450 °C; (c) 500 °C.

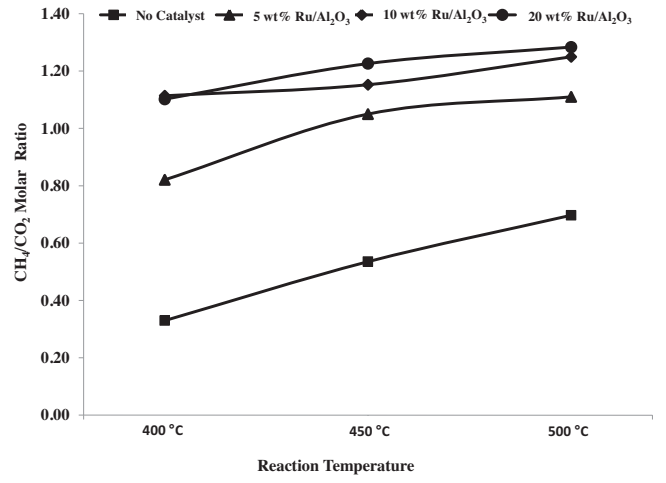

Fig. 4. CH_4/CO_2 molar ratios in relation to temperature and ruthenium loading.

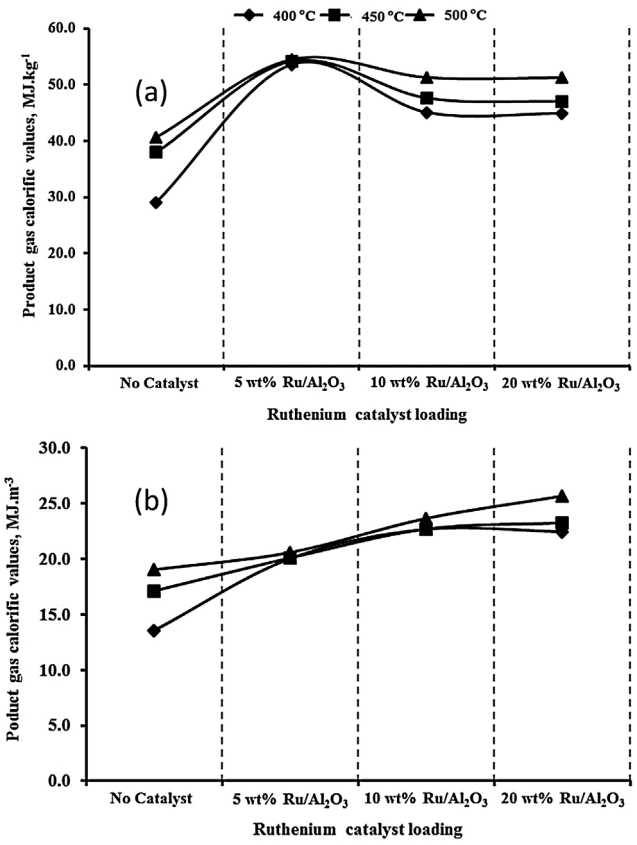

Fig. 5. Calorific values of gas products in relation temperature and ruthenium loading; (a) in MJ kg^{-1}; (b) MJ m^3.

of CO—methanation and WGS reaction [24], considering the large presence of water as reaction medium.

3.2.2.3. Calorific values of gas products. The higher heating values (HHV) of the gas products presented in Fig. 5 were estimated based on the volume percent of gas components, using the equation below;

$$\mathrm{HHV} = \sum_{i=1}^{n} x.\mathrm{CV} \quad (4)$$

where $i \ldots n$ = each combustible component in the gas product.

x = Volume fraction of gas component.

CV = Calorific value of gas component in MJ kg^{-1} (and also in MJ m^{-3}, respectively).

Fig. 5a is the calorific values in MJ kg^{-1}, which clearly shows that the calorific values of the gas products generally increased as the ruthenium oxide loading increased. The highest calorific values in Fig. 5a was obtained with the 5 wt% catalyst due to the high yields of hydrogen with this catalyst compared to catalyst with higher ruthenium loading. This is the case considering that hydrogen has a much higher calorific value per kg than the other gases. However, as shown in Fig. 5b there was a consistent rise in the energy content (per cubic metre) of the gas products with increasing ruthenium oxide loading. Clearly, the contributions to calorific value of the increasing yields CO and methane with temperature under the non-catalytic condition can be seen in this figure. However, as methanation increased, there were only slight differences in calorific values at the three different temperatures with the 5 wt% and 10 wt% catalysts. It was only with the 20 wt% catalyst that again, an increasing trend in calorific values with increasing temperature was observed.

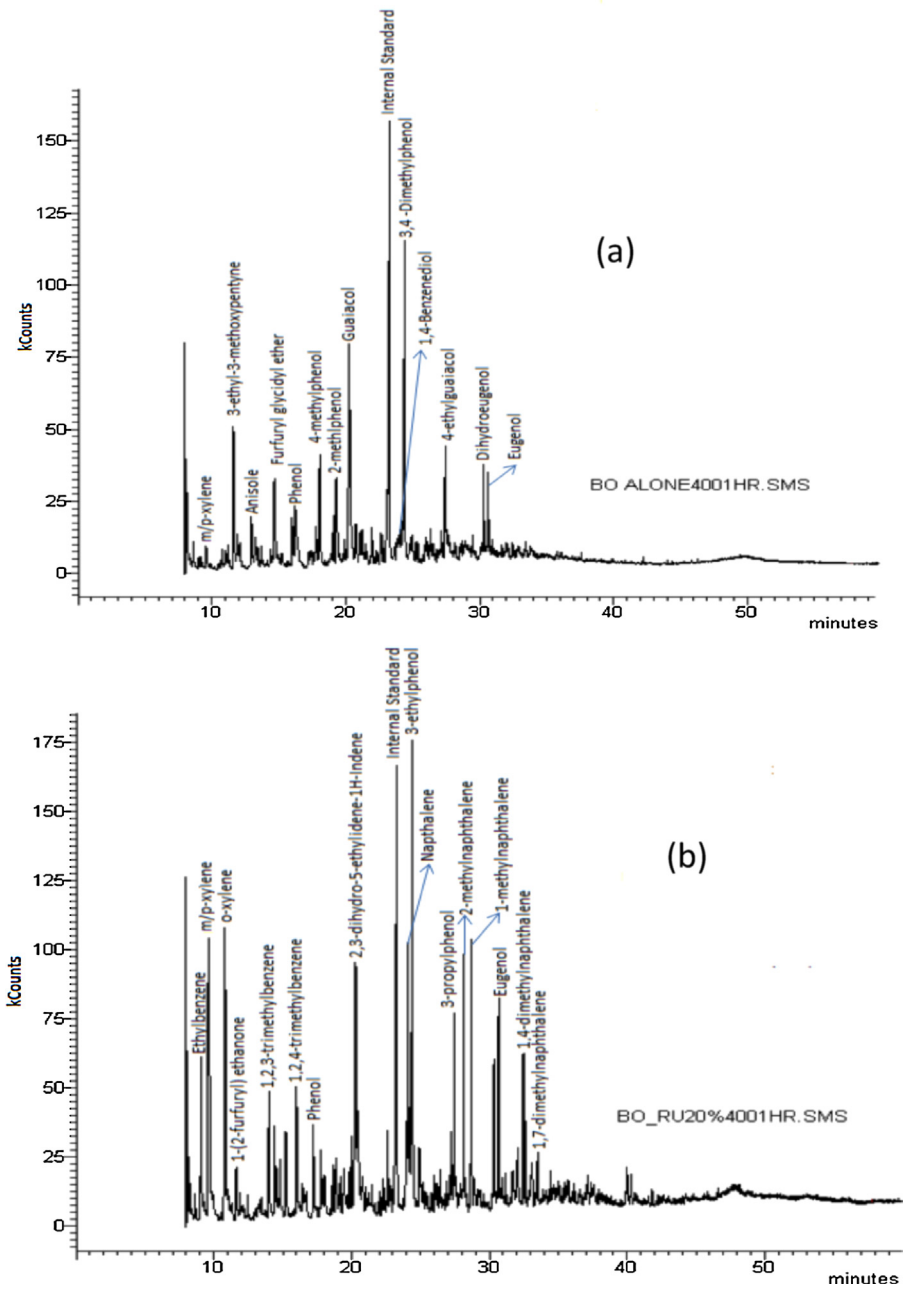

Fig. 6. GC/MS total ion chromatograms of oil products obtained at 400 °C; (a) without catalysts; (b) with 20 wt% $RuO_2/\gamma\text{-}Al_2O_3$.

3.3. Oil compositions

Although the main focus of this work was on the gas products, it was also important to present the compositions of some of the oil products obtained. In particular, significant yields of oil products were observed at 400 °C, which reached up to 31 wt% in the non-catalyzed reaction. Hence, the yields of the important components of these oils obtained from tests carried out at 400 °C are presented here. Fig. 6 presents the total ion chromatograms (TICs) of the oils obtained at 400 °C without catalyst and with the 20 wt% $RuO_2/\gamma\text{-}Al_2O_3$, which show the qualitative compositions of the oils. The oil components have been classified into aliphatics, alkylbenzenes, phenols, polycyclic aromatic hydrocarbons (PAH) and others. Aliphatic compounds included ketones, aldehydes, alcohols and carboxylic acids without the aromatic ring. The major compounds in this category included cyclopentenones, alkyl cyclopentenones, hexanal, hexanoic acid. Alkylbenzenes included ethylbenzene, xylenes, and various methylated benzenes including tri- tetra-, penta- and hexa- methyl benzenes. The class denoted as phenols included mainly phenol and alkylated phenols, particularly guaiacol which accounted for more than 50% of the phenols. The compounds identified among the class of PAH included naphthalene and alkylated naphthalenes, biphenyls, fluorene, acenaphthene and various alkylated indenes.

The yields of these classes of compounds are presented in two different ways in Fig. 7. In Fig. 7a, the yields of the compounds in relation to the bio-oil feed is presented. This figure clearly shows that the yields of compounds in the oil products decreased as the ruthenium catalyst loading increased even at 400 °C, which also mirrored the decreased in the overall oil yields. Phenols were the dominant compounds obtained during the uncatalyzed reaction at this temperature. In the presence of the 5 wt% $RuO_2/\gamma\text{-}Al_2O_3$ catalyst, the yields of phenol decreased, while yields of compounds in the other four classes increased compared to the uncatalyzed test.

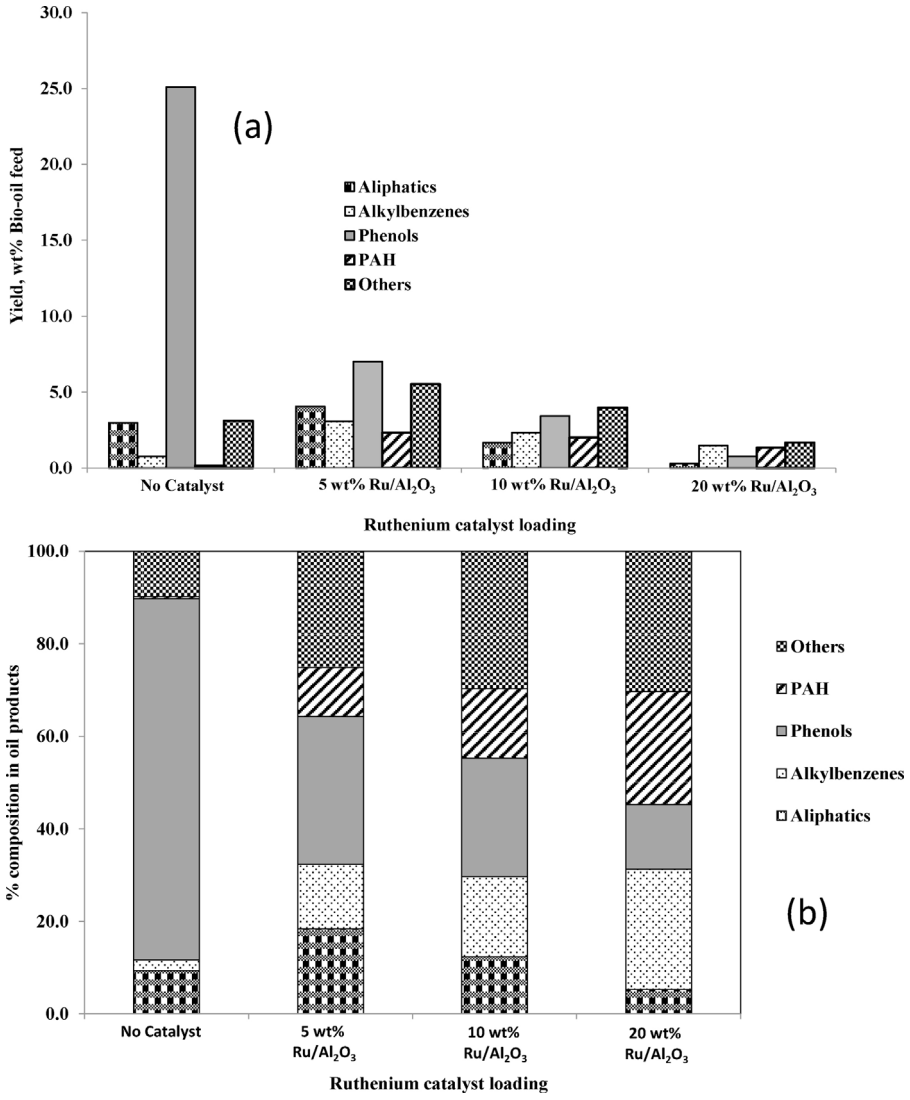

Fig. 7. Compositions of oil products obtained at 400 °C in relation to ruthenium loading (a) in wt% bio-oil; (b) relative% yields.

This suggested that the catalyst was capable of converting phenol to other less oxygenated liquid compounds and gas products. The consistent decrease in the yields of all compounds as the ruthenium loading increased, obviously indicated increased catalytic activity leading to gasification of the intermediate products. Results from the 20 wt% RuO_2/γ-Al_2O_3 catalyst clearly demonstrated that phenols were less stable than alkylbenzenes and PAH under the reaction conditions. This is confirmed from the data presented in Fig. 7b, which shows that as the ruthenium loading increased, the percentage of phenols in the oil decreased, while those of alkylbenzenes and PAH increased. This is also corroborated in the TICs shown in Fig. 6 above. The possible formation of these stable aromatic hydrocarbons from phenol could be explained by the increased yield of CO_2 in the gas phase, indicating deoxygenation or decarboxylation in the presence of ruthenium. Hence, the ruthenium catalyst could be considered to be active in catalysing carbon gasification as well as the methanation of the mainly dominant CO_2 gas product.

3.4. Analysis of used catalysts

Results of XRD analysis of some of the fresh and used catalysts (after calcination) are presented in Fig. 8, which shows that there were no appreciable changes in the phase of the ruthenium oxide in the catalyst after use in the 20 wt% catalyst. For the catalysts, with lower ruthenium oxide loading, the diffraction peaks for the oxide became more intense which may indicate structural changes in the bulk catalysts [27]. Although, not all the catalysts have been reused to test the catalytic stability, one-off tests with the 5 wt% and 20 wt% RuO_2/γ-Al_2O_3 were carried out at 450 °C for 60 min, respectively. The gas results showed only a slight decrease in methane yield to 28.2 wt% compared to methane yield with the fresh catalyst of 29.4 wt%, for the 20 wt% ruthenium catalyst, and with only slight increase (2.4 wt%) in hydrogen yield. In contrast, with the 5 wt% catalyst, methane yield showed a larger decrease of 5.5% and hydrogen yields increased by 9.6%. In a previous work [22], it was also shown that subsequent reuse of 5 wt% RuO_2/γ-Al_2O_3 led to about 5 mol% decrease in methane yields, while hydrogen yields increased by 10 mol%. Hence, it could be deduced that higher ruthenium loading ensured greater catalytic stability and activity, although more expensive. Yamamura et al. [24] also reported that un-supported RuO_2 was not deactivated during SCWG of cellulose, glucose and N-heterocyclic compounds, however slight deactivation was observed with sulphur-containing feedstocks. This stability of the 20 wt% catalyst is supported by the data from the SEM-EDXS semi-quantitative analysis presented in

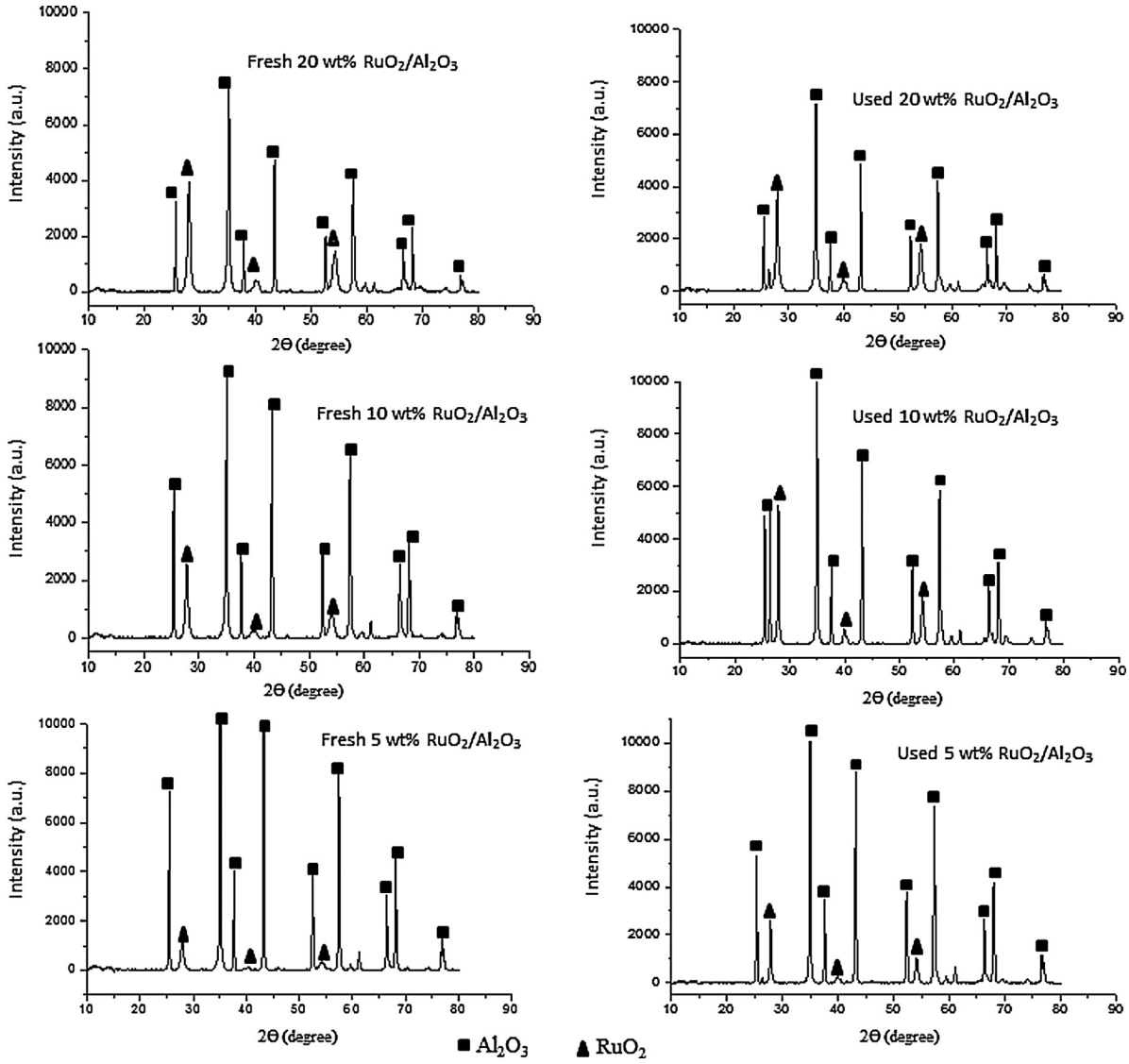

Fig. 8. Annotated XRD patterns of the fresh and used catalyst (after calcination).

Table 4
Semi-quantitative composition of the fresh, used and calcined catalysts.

		400 °C		450 °C	
Parameters	Fresh	Used	Calcined	Used	Calcined
Carbon (wt%)	–	14.9	–	16.4	–
Oxygen (wt%)	53.2	46.4	50.8	47.0	54.3
Aluminium (wt%)	31.7	27.5	34.8	26.2	30.7
Ruthenium (wt%)	15.1	11.2	14.4	10.4	15.0

Table 4, which shows the presence of carbon in the used catalyst. However, the carbon was completely removed also calcination at 550 °C overnight. The actual amounts of ruthenium in the used 20 wt% catalysts remained fairly the same and similar to the amount in the fresh catalyst earlier presented in Table 1.

4. Conclusion

In this work, the supercritical water gasification of dewatered heavy fraction of bio-oil produced from mixed softwood samples have been investigated in the presence of ruthenium oxide catalysts, with different ruthenium loadings. Results from the batch reactor tests show that ruthenium catalysts were very active in the production of methane, possibly via CO_2 methanation. Higher ruthenium loading led to increased carbon gasification efficiencies, high methane production and dramatic reduction it both char and oil yields. Detailed compositional analysis of gas products indicate that the catalytic gasification process could have included; (1) initial oxidation of bio-oil to carbon monoxide and carbon dioxide; (2) WGS shift reaction to produce hydrogen, and (3) reduction of carbon dioxide to CO followed by CO methanation. However, the presence of water also ensured competition between CO methanation and WGS reaction to produce hydrogen. In addition, high ruthenium loading resulted in higher catalytic and stability of the catalysts, so that with the 20 wt% RuO_2/γ-Al_2O_3, there was only a slight decrease in methane selectivity when the same catalyst was recovered, calcined and re-used in the bio-oil hydrothermal gasification process. These tests, carried out in a batch reactor, show that in addition to reported efficiency of ruthenium in catalysing the aqueous phase of bio-oil, it is also effective in the complete gasification of the heavy bio-oil fractions. Thus, bio-oil can simply be converted to combustible gases such as methane and hydrogen, for which there are ready markets.

References

[1] P. Grirard, J. Blin, Environmental, health and safety aspects related to pyrolysis, in: A. Bridgwater (Ed.), Fast Pyrolysis of Biomass a Handbook, 3, CPL Press, Newbury, UK, 2005, pp. 1–217.
[2] P.J. Ortiz-toral, Steam Reforming of Water-soluble Fast Pyrolysis Bio-oil: Studies on Bio-oil Composition Effect, Carbon Deposition, and Catalyst Modifications, Iowa State University, 2011, PhD Thesis. Available online. Accessed 02/03/2015.
[3] M.J. Antal, S.G. Allen, D. Schulman, X.D. Xu, R.J. Divilio, Ind. Eng. Chem. Res. 39 (2000) 4040–4053.
[4] Y. Matsumura, T. Minowa, Int. J. Hydrogen Energy 29 (2004) 701–707.
[5] Y. Matsumura, T. Minowa, B. Potic, S.R.A. Kersten, W. Prins, W.P.M. van Swaaij, B. van de Beld, D.C. Elliott, G.G. Neuenschwander, A. Kruse, M.J. Antal, Biomass Bioenergy 29 (2005) 269–292.
[6] L. Guo, C. Cao, Y. Lu, Supercritical water gasification of biomass and organic wastes, in: M. Momba, Bux Faizal (Eds.), Biomass, 202, Sciyo, Croatia, 2010, ISBN 978-953-307-113-8.
[7] Q. Zhang, J. Chang, T. Wang, Y. Xu, Energy Convers. Manage. 48 (2007) 87–92.
[8] S. Czernik, A.V. Bridgwater, Energy Fuels 18 (2004) 590–598.
[9] A.V. Bridgwater, Biomass Bioenergy 38 (2012) 68–94.
[10] M.H. Waldner, F. Vogel, Ind. Eng. Chem. Res. 44 (2005) 4543–4551.
[11] G. Van Rossum, S.R.A. Kersten, W.P.M. Van Swaaij, Ind. Eng. Chem. Res. 46 (2007) 3959–3967.
[12] G. Van Rossum, S.R.A. Kersten, W.P.M. Van Swaaij, Ind. Eng. Chem. Res. 48 (2009) 5857–5866.
[13] C. Di Blasi, C. Branca, A. Galgano, D. Meier, I. Brodzinski, O. Malmros, Biomass Bioenergy 31 (2007) 802.
[14] Q. Li, P.H. Steele, B. Mitchell, L.L. Ingram, F. Yu, BioResources 8 (2013) 1868–1880.
[15] J.M.L. Penninger, M. Rep, Int. J. Hydrogen Energy 31 (2006) 1597–1606.
[16] T.P. Vispute, G.W. Huber, Green Chem. 11 (2009) 1433–1445.
[17] A.G. Chakinala, J.K. Chinthaginjala, K. Seshan, W.P.M. van Swaaij, S.R.A. Kersten, D.W.F. Brilman, Catal. Today 195 (2012) 83–92.
[18] Y.J. Lu, L.J. Guo, C.M. Ji, X.M. Zhang, X.H. Hao, Q.H. Yan, Int. J. Hydrogen Energy 31 (2006) 822–831.
[19] R. Muangrat, J.A. Onwudili, P.T. Williams, Int. J. Hydrogen Energy 37 (2012) 2248–2259.
[20] R. Cherad, J.A. Onwudili, P.T. Williams, A.B. Biores, Biores. Technol. 169 (2014) 573–580.
[21] J.A. Onwudili, Biores. Technol. 187 (2015) 60–69.
[22] J.A. Onwudili, P.T. Williams, Appl. Catal. B 132–133 (2013) 70–79.
[23] J.A. Onwudili, M.A. Nahil, C. Wu, P.T. Williams, RSC Adv. 4 (2014) 34784–34792.
[24] T. Yamamura, T. Mori, K.C. Park, Y. Fujii, H. Tomiyasu, J. Supercrit. Fluids 51 (2009) 43–49.
[25] T. Sato, M. Osada, M. Watanabe, M. Shirai, K. Arai, Ind. Eng. Chem. Res. 42 (2003) 4277–4282.
[26] A.J. Byrd, K.K. Pant, R.B. Gupta, Ind. Eng. Chem. Res. 46 (2007) 3574–3579.
[27] L. Chen, Y. Zhu, H. Zheng, C. Zhang, B. Zhang, Y. Li, J. Mol. Catal. A 351 (2011) 217–227.
[28] D.C. Elliott, T.R. Hart, A.J. Schmidt, G.G. Neuenschwander, L.J. Rotness, M.V. Olarte, A.H. Zacher, K.O. Albrecht, R.T. Hallen, J.E. Holladay, Algal Res. 2 (2013) 445–454.
[29] A.J. Byrd, Hydrogen Production in Supercritical Water, Auburn University, Alabama, USA, 2015, PhD Thesis. Available online accessed 06/03/2015.
[30] F.S. Karn, J.F. Shultz, R.B. Anderson, Ind. Eng. Chem. Prod. Res. Dev. 5 (1965) 265–269.
[31] P.J. Lunde, F.L. Kester, J. Catal. 30 (1973) 423–429.